The 9^+-Intersection for Topological Relations between a Directed Line Segment and a Region

Yohei Kurata[1] and Max J. Egenhofer[2]

[1] SFB/TR8 Spatial Cognition, Universität Bremen
Postfach 330 440, 28334 Bremen, Germany
ykurata@informatik.uni-bremen.de

[2] National Center for Geographic Information and Analysis, and
Department of Spatial Information Science and Engineering,
University of Maine
Boardman Hall, Orono, ME 04469-5711, USA
max@spatial.maine.edu

Abstract. This paper develops a formal model of topological relations between a directed line segment (*DLine*) and a region in a two-dimensional space. Such model forms a foundation for characterizing movement patterns of an agent with respect to a region. The DLine-region relations are captured by the 9-intersection for line-region relations with further distinction of the line's boundary into two subparts (starting and ending points). This *9^+-intersection* distinguishes 26 topological DLine-region relations. The relations' conceptual neighborhood graph takes the shape of a V-shaped tube, whose upper and lower halves are isomorphic to the conceptual neighborhood graph of 19 topological line-region relations. The conceptual neighborhood graph of the 26 DLine-region relations is applied to the iconic representation of movement patterns that satisfy a qualitative condition. By manipulating such iconic representations, the movement patterns that satisfy complex conditions are easily deduced.

1. Introduction

Movement of an agent with respect to an area, such as *entering*, *leaving*, and *going-through*, is modeled as a spatial relation between a directed line segment and a region. For instance, Figs. 1a and 1b illustrate two scenarios, *going abroad from Germany* and *being blocked by the cell wall*, by the combinations of a directed line segment and a region with different spatial relations. Similarly, how a person goes in and out of a room, a hazardous district, or any area of interest, is captured as a spatial relation between a directed line segment and a region. Among several types of spatial relations, topological relations are particularly important, because the topological relations capture how the agent moves between the inside and outside and how the agent crosses or touches the border, which are fundamental information when people conceptualize the movement. A model of such topological relations is, therefore, potentially useful for the information systems that concern spatio-dynamic behaviors, such as security monitoring systems, smart homes, mobile robots, and route navigation systems, where computers have to communicate qualitative information about spatial movement patterns with human users.

(a) (b)

Fig. 1. (a) A directed line segment starts from the inside and ends at the outside of a Germany-shaped region, illustrating *going abroad from Germany*. (b) A directed line segment starts from the outside, touches the boundary, and ends at the outside of a cell-shaped region, illustrating *being blocked by the region.*

The goal of this paper is to develop a formal model of topological relations between a directed line segment and a region embedded in a two-dimensional space. Spatial relations between a directed line segment and a region, including topological relations, have not systematically studied, even though there are many studies on spatial relations between two directed line segments (Schlieder 1995; Clementini and Di Felice 1998; Moratz *et al.* 2000; Kurata and Egenhofer 2006) and those between a non-directed line segment and a region (Egenhofer and Herring 1991; Mark and Egenhofer 1994). Our model, which stands on these existing studies, distinguishes a set of topological relations between a directed line segment and a region in a formal way. This relation set forms a foundation for characterizing the movement patterns of an agent with respect to a region.

A non-branching, non-directed line segment is often called a *line* for short (Egenhofer and Herring (1991), Hadzilacos and Tryfona (1992), Clementini (1993), Paradias (1995), Schlieder (1995), Clementini (1998), Moratz (2000)). In contrast, this paper calls a non-branching directed line segment a *DLine* (Kurata and Egenhofer 2006). Accordingly, a spatial relation between a DLine and a region is called a *DLine-region relation.*

The remainder of this paper is structured as follows: Section 2 reviews related work on topological relations. Section 3 develops a formal model of topological DLine-region relations. Based on this model Section 4 identifies the complete set of DLine-region relations in a two-dimensional space, which are then schematized by a conceptual neighborhood graph in Section 5. Section 6 applies the conceptual neighborhood graph to the iconic representation of the movement patterns that satisfy certain qualitative conditions and demonstrates some benefits of this representation. Finally, Section 7 concludes with a discussion of future problems.

2. Related Work

Topological relations are spatial relations that are invariant under topological transformations, such as translation, rotation, and scaling (Egenhofer 1989). Topological relations are considered highly influential for people's conceptualizations of space (Lynch 1960; Egenhofer and Mark 1995b). Topological relations between two spatial objects (i.e., points, lines, and regions) and their lower-dimensional counterparts, time intervals, have been studied extensively, starting from Allen's (1983) thirteen interval relations. Based on the point-set topology (Alexandroff 1961), the *4-intersection* (Egenhofer and Franzosa 1991) formally captures topological relations between two spatial objects through the geometric intersections of the objects' interiors and boundaries. The *9-intersection* (Egenhofer and Herring 1991) further considers the intersections with respect to the objects' exteriors. In this model, topological relations between two spatial objects *A* and *B* are characterized by the *9-intersection matrix* (Eqn. 1), where A°, ∂A, and A^- are *A*'s interior, boundary, and exterior while B°, ∂B, and B^- are *B*'s interior, boundary, and exterior, respectively. Based on the presence or absence of the 3×3 types of geometric intersections, the 9-intersection distinguishes 19 topological relations between a line and a region in $\mathbf{R}^2$ (Egenhofer and Herring 1991) and 43 topological relations between a complex line and a complex region in $\mathbf{R}^2$ (Schneider and Behr 2006).

$$M(A,B) = \begin{pmatrix} A^\circ \cap B^\circ & A^\circ \cap \partial B & A^\circ \cap B^- \\ \partial A \cap B^\circ & \partial A \cap \partial B & \partial A \cap B^- \\ A^- \cap B^\circ & A^- \cap \partial B & A^- \cap B^- \end{pmatrix} \qquad \textbf{(1)}$$

Another variation of the 4-intersection distinguishes explicitly the disconnected subparts of the interval's boundary or DLine's boundary (i.e., its starting point and ending point), distinguishing 16 relations between two intervals in a temporal cycle (Hornsby *et al.* 1999) and 68 relations between two DLines in $\mathbf{R}^2$ (Kurata and Egenhofer 2006).

A set of spatial relations is typically schematized by a *conceptual neighborhood graph* (Egenhofer and Al-Taha 1992; Freksa 1992a; Egenhofer and Mark 1995b; Papadias *et al.* 1995; Schlieder 1995; Hornsby *et al.* 1999; Egenhofer 2005; Van de Weghe and De Maeyer 2005; Kurata and Egenhofer 2006). In this graph, each node corresponds to a spatial relation and two nodes are linked if the corresponding relations are *conceptual neighbors* (Freksa 1992a). Different definitions of conceptual neighbors lead to different graphs. For instance, Egenhofer and Mark (1995a) derived two different conceptual neighborhood graphs of the 19 line-region relations based on the *smooth-transition* (Freksa 1992a), which requires the possibility of continuous transformation between the neighboring relations, and the *minimum topological distance* (Egenhofer and Al-Taha 1992), which requires minimum difference between the 9-intersection matrices of the neighboring relations.

The conceptual neighborhood graph has been applied to the analysis of spatial predicates in natural languages (Mark and Egenhofer 1994; Sharif *et al.* 1998). These linguistic studies show that line-region relations are often associated with a spatial predicate that assumes a spatial movement along the line, such as *going into*. This implies that people may recognize a line segment by imposing a virtual movement on it, despite the lack of the line's direction, just like such verbal expressions as "*the mountain range goes from Mexico to Canada*" evokes *fictive motion* (Talmy 1996).

3. The 9^+-intersection for Topological DLine-Region Relations

This paper considers DLines that may curve, but have no loop. Such DLines are *simple lines* with direction, which is obtained through a continuous one-to-one mapping from [0, 1] to $\mathbf{R}^2$ (Schneider and Behr 2006). In the point-set topology (Alexandroff 1961), a simple line is considered a set of an infinite number of linearly aligned points, among which two distinctive end-points form the *boundary* and the other points form the *interior*. The *exterior* is the complement of the union of the boundary and the interior. Naturally, the interior, boundary, and exterior of a DLine are pairwise disjoint and jointly exhaustive in $\mathbf{R}^2$. A DLine categorizes its two end-points into a *starting point* and an *ending point*, which are also called a *tail* and a *head*, respectively (Kurata and Egenhofer 2006).

A *single-component region* is a connected, homogeneously two-dimensional 2-cell in $\mathbf{R}^2$ (Schneider and Behr 2006). A single-component region does not have two or more disconnected interiors, spikes, puncturing points, cuts, but may have holes. A *multi-component region* is the union of multiple disjoint single-component regions. In this paper, a *region* refers to a single-component region or a multi-component region. The interior, boundary, and exterior of a region are pairwise disjoint and jointly exhaustive in $\mathbf{R}^2$.

Let *D* and *R* be a DLine and a region, respectively. Uppercase letters are used because they are considered point sets. In the 9-intersection (Egenhofer and Herring 1991) their topological relation is captured through the geometric intersections of *D*'s three topological parts (i.e., interior D°, boundary ∂D, and exterior D^-) and *R*'s three topological parts (i.e., interior R°, boundary ∂R, and exterior R^-). These 3×3 types of intersections are concisely represented by the 9-intersection matrix in Eqn. 2.

$$M(D,R)=\begin{pmatrix} D^\circ \cap R^\circ & D^\circ \cap \partial R & D^\circ \cap R^- \\ \partial D \cap R^\circ & \partial D \cap \partial R & \partial D \cap R^- \\ D^- \cap R^\circ & D^- \cap \partial R & D^- \cap R^- \end{pmatrix} \tag{2}$$

In our model, the intersections with respect to *D*'s boundary ∂D are further distinguished into the intersections with respect to *D*'s starting point $\partial_s D$ and those with respect to *D*'s ending point $\partial_e D$. Accordingly, the 9-intersection matrix in Eqn. 2 is extended to the matrix in Eqn. 3, which is called the *9^+-intersection matrix* of the topological relation between the DLine *D* and the region *R*.

$$M^+(D,R)=\begin{pmatrix} D^\circ \cap R^\circ & D^\circ \cap \partial R & D^\circ \cap R^- \\ \begin{bmatrix} \partial_s D \cap R^\circ \\ \partial_e D \cap R^\circ \end{bmatrix} & \begin{bmatrix} \partial_s D \cap \partial R \\ \partial_e D \cap \partial R \end{bmatrix} & \begin{bmatrix} \partial_s D \cap R^- \\ \partial_e D \cap R^- \end{bmatrix} \\ D^- \cap R^\circ & D^- \cap \partial R & D^- \cap R^- \end{pmatrix} \tag{3}$$

In general, the 9^+-intersection captures topological relation between two spatial objects *A* and *B* through the geometric intersections of all subparts of *A*'s interior, boundary, and exterior and all subparts of *B*'s interior, boundary, and exterior. The subparts of the interior, boundary, and exterior are determined by their disconnections. For instance, a single-component region with n holes has $n + 1$ boundary subparts and $n + 1$ exterior subparts. On the other hand, we consider that a connected interior, boundary, or exterior consists of a single subpart. Accordingly, Eqn. 4 is the general form of the 9^+-intersection matrix, where A°_i}, $\partial_i A$, and A^{-_i} are the i-th subpart of A's interior, boundary, and exterior while B°_j}, $\partial_j B$, and B^{-_j} are the j-th subpart of B's interior, boundary, and exterior, respectively.

$$M^+(A,B) = \begin{pmatrix} \left[A^{\circ_i} \cap B^{\circ_j}\right] & \left[A^{\circ_i} \cap \partial_j B\right] & \left[A^{\circ_i} \cap B^{-_j}\right] \\ \left[\partial_i A \cap B^{\circ_j}\right] & \left[\partial_i A \cap \partial_j B\right] & \left[\partial_i A \cap B^{-_j}\right] \\ \left[A^{-_i} \cap B^{\circ_j}\right] & \left[A^{-_i} \cap \partial_j B\right] & \left[A^{-_i} \cap B^{-_j}\right] \end{pmatrix} \quad \textbf{(4)}$$

For instance, the DLine-region relation in Fig. 2b and the DLine-DLine relation in Fig. 2c are captured by the 9^+-intersection matrix shown in each figure.

For simplification, the 9^+-intersection matrices are represented by icons (Fig. 2b-2c). These icons are based on the iconic representation of the 9-intersection matrix by Mark and Egenhofer (1994) (Fig. 2b). Each icon has 3×3 cells, which correspond to the matrix's 3×3 elements. Each cell is marked out if the corresponding element is non-empty ($\neg\phi$). In our iconic representation, the icon's columns and rows are partitioned if their corresponding topological parts have multiple subparts. For instance, when visualizing the 9^+-intersection matrix of a DLine-region relation, the icon's second row is partitioned (Fig. 2b), such that the upper and lower halves correspond to the intersections with respect to the DLine's starting point and ending point, respectively. Similarly, for a DLine-DLine relation, both the second row and the second column of the icon are partitioned (Fig. 2c).

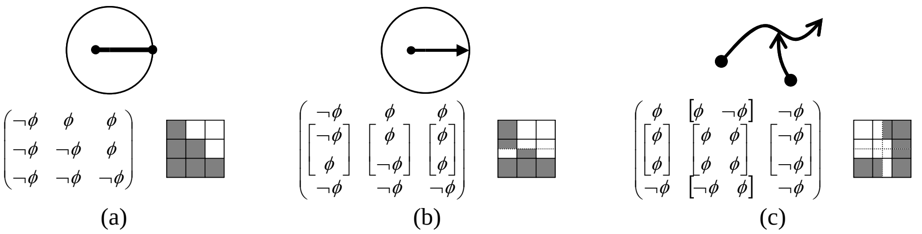

Fig. 2. Sample configurations of (a) a line and a region, (b) a DLine and a region, and (c) two DLines, together with (a) the 9-intersection and (b-c) the 9^+-intersection matrices which capture their topological relations. The icons visualize the pattern of these matrices.

4. Set of Topological DL-Region Relations

From the 19 topological line-region relations distinguished by the 9-intersection (Egenhofer and Herring 1991) we can derive a set of topological DLine-region relations through assigning directions to the lines. Among the 19 relations, twelve relations (Figs. 3a-l) are invariant to the line's direction, because the line's two end-points are located at the same part of the region, whereas seven relations (Fig. 3m-s) are variant to the line's direction. From each direction-variant relation we can derive two DLine-region relations through assigning different directions to the line. As a result, $12 + 7 \times 2 = 26$ topological DLine-region relations are obtained (Fig. 4).

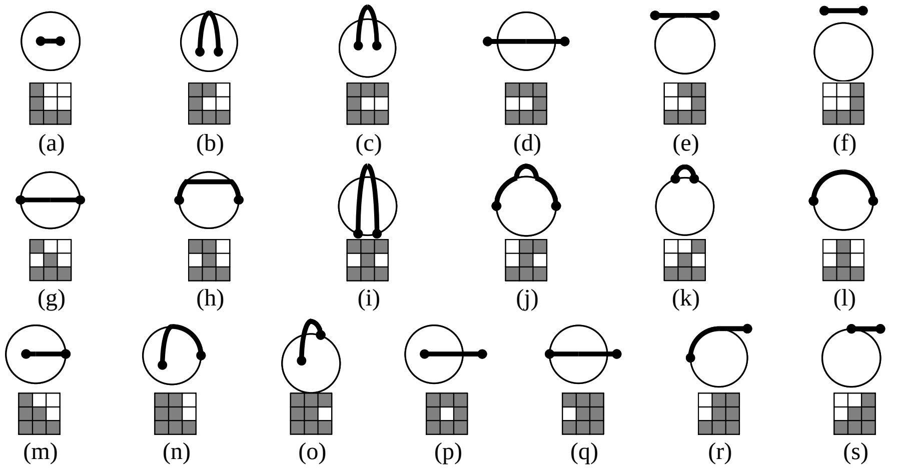

Fig. 3. Sample configurations of 19 topological line-region relations (Egenhofer and Herring 1991), together with the patterns of the corresponding 9-intersection matrices.

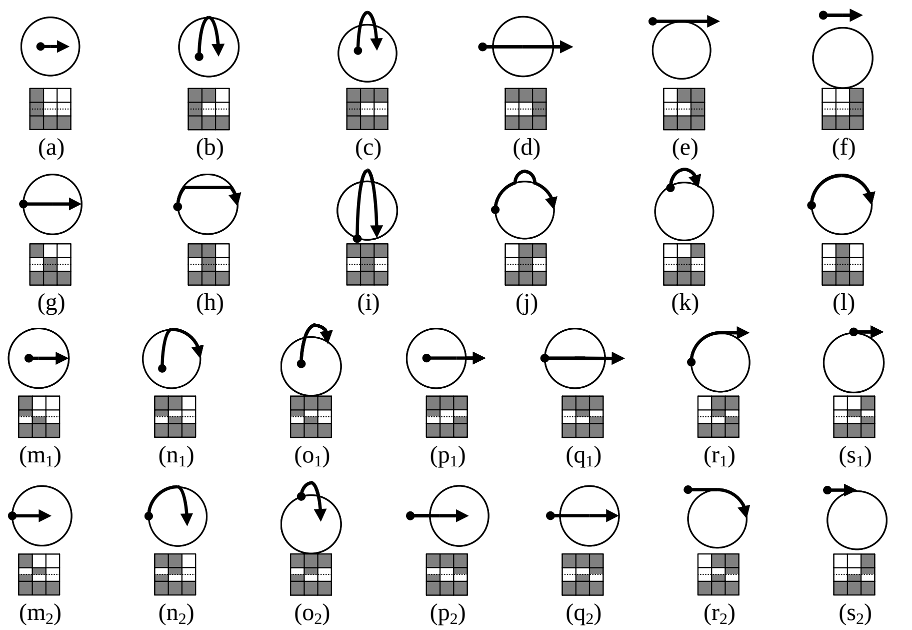

Fig. 4. Sample configurations of 26 topological DLine-region relations, together with the patterns of the corresponding 9^+-intersection matrices.

These 26 relations correspond to different patterns of the 9^+-intersection matrices (Fig. 4). This indicates that the 9^+-intersection distinguishes *at least* 26 DLine-region relations. Actually, there is no other DLine-region relation that the 9^+-intersection distinguishes. This is proven with the aid of the constraints on the 9^+-intersection matrix of DLine-region relations (Eqns. 6-14), which are derived systematically from the constraints on the 9-intersection matrix of line-region relations (Egenhofer and Herring 1991) considering the distinction of lines' two end-points.

- D's exterior and R's exterior intersect with each other.

$$D^- \cap R^- = \neg\phi \tag{5}$$

- If D's interior is a subset of R's closure then D's both end-points must be a subset of R's closure as well.

$$D^\circ \cap R^- = \phi \quad \rightarrow \quad \partial_s D \cap R^- = \phi \quad \wedge \quad \partial_e D \cap R^- = \phi \tag{6}$$

- D's each end-point intersects at least one part of R.

$$\exists P, Q \in \{R^\circ, \partial R, R^-\} \quad \partial_s D \cap P = \neg\phi \quad \wedge \quad \partial_e D \cap Q = \neg\phi \tag{7}$$

- If D's interior and R's interior are disjoint then neither of D's end-points can intersect with R's interior.

$$D^\circ \cap R^\circ = \phi \quad \rightarrow \quad \partial_s D \cap R^\circ = \phi \quad \wedge \quad \partial_e D \cap R^\circ = \phi \tag{8}$$

- If D's interior intersects with both R's interior and exterior, then it must also intersect with R's boundary.

$$D^\circ \cap R^\circ = \neg\phi \quad \wedge \quad D^\circ \cap R^- = \neg\phi \quad \rightarrow \quad D^\circ \cap \partial R = \neg\phi \tag{9}$$

- D's each end-point intersects one part of R.

$$\begin{aligned} &\exists P_1 \in \{R^\circ, \partial R, R^-\}, \forall Q_1 \in \{R^\circ, \partial R, R^-\} \setminus P_1 \quad \partial_s D \cap P_1 = \neg\phi \quad \wedge \quad \partial_s D \cap Q_1 = \phi \\ &\exists P_2 \in \{R^\circ, \partial R, R^-\}, \forall Q_2 \in \{R^\circ, \partial R, R^-\} \setminus P_2 \quad \partial_e D \cap P_2 = \neg\phi \quad \wedge \quad \partial_e D \cap Q_2 = \phi \end{aligned} \tag{10}$$

- R's interior always intersects with D's exterior.

$$D^- \cap R^\circ = \neg\phi \tag{11}$$

- R's boundary always intersects with D's exterior.

$$D^- \cap \partial R = \neg\phi \tag{12}$$

- D's interior must intersects with at least one part of R.

$$\exists P \in \{R^\circ, \partial R, R^-\} \quad D^\circ \cap P = \neg\phi \tag{13}$$

The 9^+-intersection matrix may have $2^{12} = 4096$ patterns, since it has 12 elements with two possible values (empty or non-empty). Among these 4096 patterns, however, only 26 patterns satisfy the constraints in Eqns. 6-14. These 26 patterns are exactly same as the matrix patterns in Fig. 4. This indicates that the 26 patterns in Fig. 4 are the complete set of topological DLine-region relations distinguished by the 9^+-intersection.

In Fig. 4, the geometric configuration assigned to each DLine-region relation is merely an example. It is possible that other configurations, which are topologically different from the illustrated example, may also correspond to the same topological relation (Fig. 5). In this sense, the 26 topological relations categorize DLine-region configurations based on some topological characteristics (the presence or absence of 12 types of intersections), but not on their topological equivalence.

To describe the topological detail of DLine-region configurations, this paper also introduces an alternative notation by three-tuples, which trace the positions of a virtual agent moving along the DLine (Fig. 5a-c). The first and third element in each three-tuple represents the agent's starting and ending positions, while the second element represents the sequence of the agent's intermediate positions. *I*, *B*, *E* represent the positions in the region's interior, boundary, and exterior, respectively.

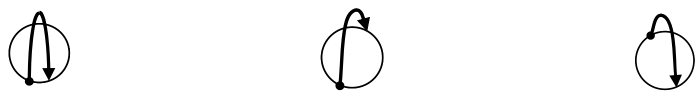

(a) $(B, IBEBI, B)$ (b) (B, IBE, B) (c) (B, EBI, I)

Fig. 5. Three configurations that correspond to the same DLine-region relation in Fig. 4i.

With such three-tuple notations, Table 1 summarizes all DLine-region configurations that belong to the 26 DLine-region relations. This table indicates that 17 DLine-region relations correspond to multiple configurations (i.e., they have multiple topological interpretations).

Table 1. Sets of DLine-region configurations that belong to each DLine-region relations in Fig. 4. Each set of configurations is described using the three-tuple notation, where $[X]$ is an empty or X, Y^* is an arbitrary number of Y, and $Z|W$ is Z or W, but not both.

<table>
<tr><th colspan="2">Direction-Invariant Relations</th><th colspan="2">Direction-Variant Relations</th></tr>
<tr><td>(a)</td><td>(I, I, I)</td><td>(m_1)</td><td>(I, I, B)</td></tr>
<tr><td>(b)</td><td>$(I, IB[IB]^*I, I)$</td><td>(m_2)</td><td>(B, I, I)</td></tr>
<tr><td>(c)</td><td>$(I, IB[IB|EB]^*E[BI|BE]^*BI, I)$</td><td>$(\mathrm{n}_1)$</td><td>$(I, IB[IB]^*[I], B)$</td></tr>
<tr><td>(d)</td><td>$(E, EB[IB|EB]^*I[BI|BE]^*BE, E)$</td><td>$(\mathrm{n}_2)$</td><td>$(B, [I][BI]^*BI, I)$</td></tr>
<tr><td>(e)</td><td>$(E, EB[EB]^*E,E)$</td><td>(o_1)</td><td>$(I, IB[IB|EB]^*E[BI|BE]^*[B], B)$</td></tr>
<tr><td>(f)</td><td>(E, E, E)</td><td>(o_2)</td><td>$(B, [B][IB|EB]^*E[BI|EI]^*BI, I)$</td></tr>
<tr><td>(g)</td><td>(B, I, B)</td><td>(p_1)</td><td>$(I, IB[IB|EB]^*E, E)$</td></tr>
<tr><td>(h)</td><td>$(B, [B]IB[IB]^*, B), (B, [BI]^*BI[B], B)$</td><td>$(\mathrm{p}_2)$</td><td>$(E, E[BI|BE]^*BI, I)$</td></tr>
<tr><td>(i)</td><td>$(B, [B][IB|EB]^*(IBE|EBI)[BI|BE]^*[B], B)$</td><td>$(\mathrm{q}_1)$</td><td>$(B, [B][IB|EB]^*I[BI|BE]^*BE, E)$</td></tr>
<tr><td>(j)</td><td>$(B, [B]EB[EB]^*, B), (B, [BE]^*BE[B], B)$</td><td>$(\mathrm{q}_2)$</td><td>$(E, EB[IB|EB]^*I[BI|BE]^*[B], B)$</td></tr>
<tr><td>(k)</td><td>(B, E, B)</td><td>(r_1)</td><td>$(B, [E][BE]^*BE, E)$</td></tr>
<tr><td>(l)</td><td>(B, B, B)</td><td>(r_2)</td><td>$(E, EB[EB]^*[E], B)$</td></tr>
<tr><td></td><td></td><td>(s_1)</td><td>(B, E, E)</td></tr>
<tr><td></td><td></td><td>(s_2)</td><td>(E, E, B)</td></tr>
</table>

5. Conceptual Neighborhood Graphs for DL-Region Relations

We schematize the 26 DLine-region relations graphically, using a *conceptual neighborhood graph* (Freksa 1992a). In this graph, each node corresponds to a spatial relation, and two nodes are linked if the corresponding relations are similar relations called *conceptual neighbors*. This paper considers that two DLine-region relations are neighbors if one relation can be derived from another relation by moving either starting point, interior, or ending point of the DLine while keeping the presence or absence of the intersections with respect to the others (Fig. 6a). This transformation is a subset of the *smooth transitions* (Egenhofer and Mark 1995a), which also includes the transformation by moving one part of the DLine without keeping the presence or absence of the intersections with respect to the others (Fig. 6b).

Fig. 6. Smooth transitions between two DLine-region relations, derived by moving the DLine's ending point from the region's boundary to (a) interior and (b) exterior, respectively. In (b), the movement of the DLine's ending point generates the intersection of the DLine's interior and the region's boundary.

We identified 46 pairs of conceptual neighbors among the 26 DLine-region relations. By linking these neighbors, a conceptual neighborhood graph of the 26 topological DLine-region relations is developed (Fig. 7). The graph is non-planar and drawn three-dimensionally on a V-shaped tube, such that links do not cross. Clearly, this graph schematizes DLine-region relations based on their similarity.

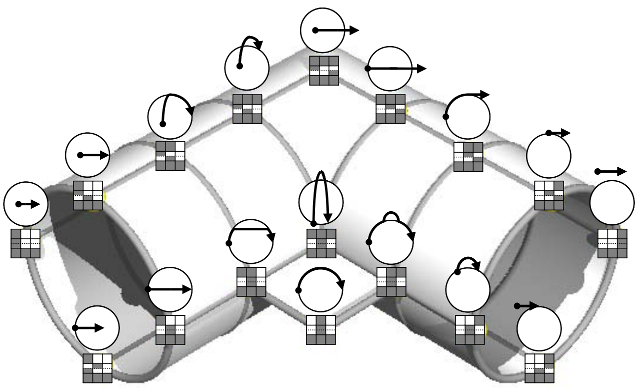

Fig. 7. A conceptual neighborhood graph of the 26 topological DLine-regions.

Fig. 8 shows the upper and lower halves of the conceptual neighborhood graph in Fig. 7. The relations with gray background in Fig. 8 correspond to the relations located at the top and bottom of the V-shaped tube in Fig. 7, respectively. Interestingly, the two subgraphs in Fig. 8 are isomorphic to the conceptual neighborhood graph of the 19 line-region relations (Fig. 9). Actually, the two subgraphs in Fig. 8 can be derived from the graph in Fig. 9 through assigning directions to the line in each relation. Since the line-region relations with gray background in Fig. 9 are variant to the line's direction, different directions assigned to the lines yield different conceptual neighborhood graphs.

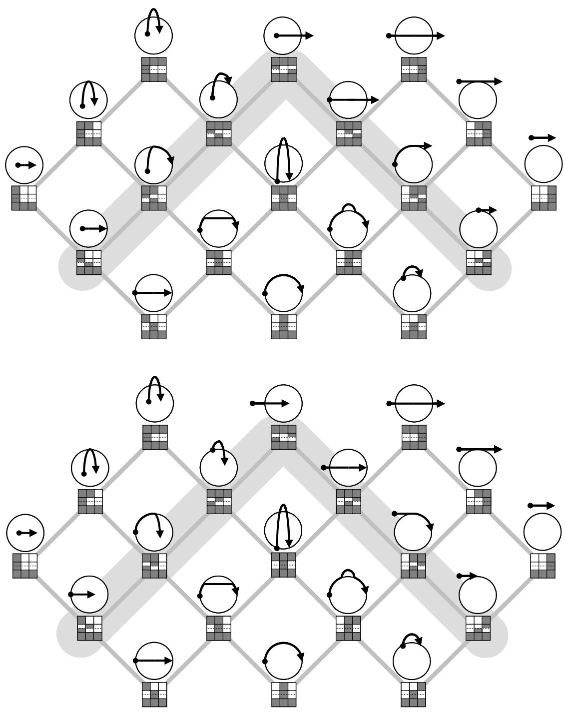

Fig. 8. Upper and lower halves of the conceptual neighborhood graph in Fig. 7. The relations with gray background correspond to the relation located at the top and bottom of the graph in Fig. 7, respectively.

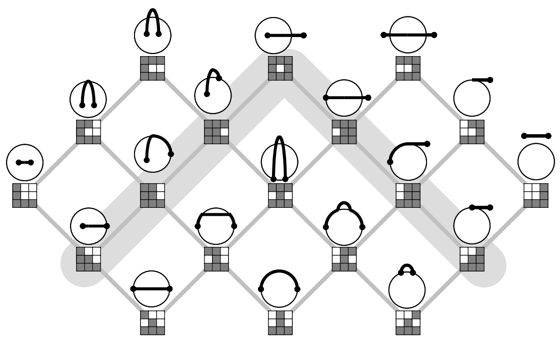

Fig. 9. The conceptual neighborhood graph of the 19 line-region relations, derived under the same definition of conceptual neighbors. The relations with gray background are variant to the line's direction.

The conceptual neighborhood graph of the 26 DLine-Region relations in Fig. 7 has the following unique properties:

- Pairs of vertically facing relations are derived from each other by exchanging upper and lower halves of the second row of the 9^+-intersection matrices (essentially reversing the DLine's direction).
- Pairs of relations located symmetrically across the front-to-back line penetrating the V-tube's center are derived from each other by flipping the 9^+-intersection matrices horizontally (essentially reversing the region's interior and exterior).
- The number of different elements in the 9^+-intersection matrix, called the *topological distance* (Egenhofer and Al-Taha 1992), is 1 between the horizontal neighbors and 2 between the other neighbors. This implies that the conceptual neighborhood graph in Fig. 7 cannot be obtained through linking all pairs of relations with minimum topological distance.

6. Modeling Movement Patterns with Respect to a Region

Topological DLine-region relations categorize the patterns of an agent's movement with respect to a region. For instance, the DLine-region relation in Fig. $4p_1$ corresponds to movement patterns that start from the region's interior, cross the region's boundary at least once, and end at the region's exterior. Such categorization is useful, because it highlights the topological characteristic of movement which highly influences people's conceptualization of movement, while abstracts less important detail. Another benefit of such categorization is that movement patterns that satisfy a certain qualitative condition, whose number is typically infinite, are captured by a finite set of DLine-region relations. For instance, a set of movement patterns that satisfy the qualitative condition, *starting from the region's interior*, is represented by the set of seven DLine-region relations (Figs. 4a, 4b, 4c, $4m_1$, $4n_1$, $4o_1$, and $4p_1$). Such summarized expression makes it easy for computers to process people's characterization of movement patterns.

To visually represent a set of DLine-region relations, we introduce iconic representations (Figs. 10a-h), which superimpose the two subgraphs in Fig. 8. The set of marked nodes indicates the set of DLine-region relations. Some nodes are partitioned, such that their upper and lower halves correspond to the different relations in the upper and lower subgraphs at the same position (i.e., the relations located at the top and bottom of the V-shaped tube in Fig. 7). For instance, the icon in Fig. 10a shows the set of seven relations in Fig. 4a, 4b, 4c, $4m_1$, $4n_1$, $4o_1$, and $4p_1$, which corresponds to the previous condition, *starting from the region's interior*. Here we consider ten basic qualitative conditions: (a) *starting from interior*, (b) *starting from boundary*, (c) *starting from exterior*, (d) *crossing boundary*, (d) *ending at interior*, (e) *ending at boundary*, (f) *ending at exterior*, and (g) *crossing/touching boundary*. The icons in Figs. 10a-h show the sets of DLine-region relations that represent all movement patterns satisfying each of these conditions.

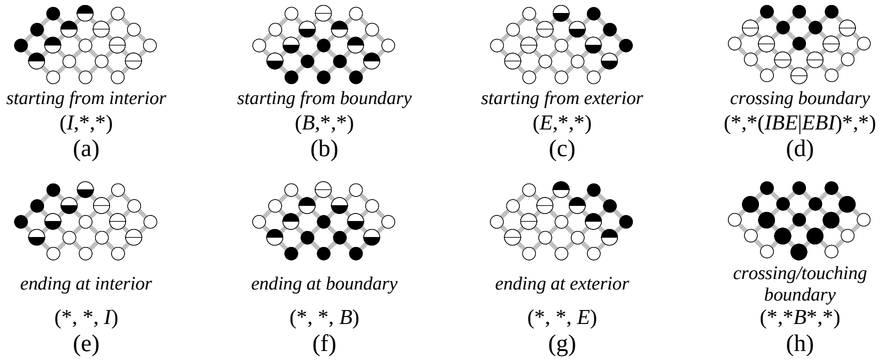

Fig. 10. Marked nodes in each icon indicate the set of DLine-region relations that represent all movement patterns satisfying each qualitative condition. Each condition is also described by the three-tuple notation (Section 4) with a wildcard symbol *.

The ten icons in Fig. 10a-h have the following unique properties:

- DLine-region relations that correspond to each qualitative condition form a connected subgraph. This is because the movement patterns that satisfy each condition has certain topological similarity, while the conceptual neighborhood graph schematizes the DLine-region relations based on their topological similarities.
- A non-directed condition, such as *crossing boundary*, yields a symmetric icon (Figs. 10d and 10h).
- A pair of conditions, interchangeable by exchanging *starting from* and *ending at* yield a pair of icons with reversed partitions (Figs. 10a and 10e, Figs. 10b and 10f, and Figs. 10c and 10g).
- A pair of conditions, interchangeable by exchanging *interior* and *exterior*, yields a pair of horizontally flipped icons with reversed partitions (Figs. 10a and 10c, and Figs. 10e and 10g).

A merit of this iconic representation is that the set of movement patterns that satisfy a complex condition is derived through simple manipulations on the icons. For instance, Fig. 11a shows the intersection of the icons in Figs. 10a and 10g, whose result indicates that only one DLine-region relation corresponds to the movement patterns satisfying *starting from interior and end at exterior* (Fig. 4p_1). Similarly, Figs. 11b-d show the union of two icons, the difference of two icons, and the complement of an icon, whose result correspond to the movement patterns satisfying *starting from inside or ending at outside*, *starting from inside but not ending at outside*, and *not starting from inside*, respectively. Such computation is particularly useful for integrating the qualitative characterizations of a movement pattern reported by multiple observers (e.g., different sensors).

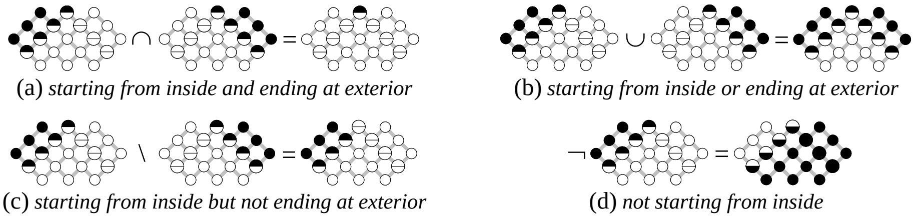

Fig. 11. Set operations on the icons for representing a set of DLine-region relations.

The iconic representation is also applicable to the classification of the region's boundary. For instance, the icon in Fig. 12a corresponds to an inapproachable boundary, like a prison's wall, which people normally cannot cross or even stand on. Conversely, the icon in Fig. 12e corresponds to a freely crossable boundary, like the border between a city square and roads around the square. In this way, the regions' boundaries can be graphically classified in terms of the movement patterns they accept (Fig. 12).

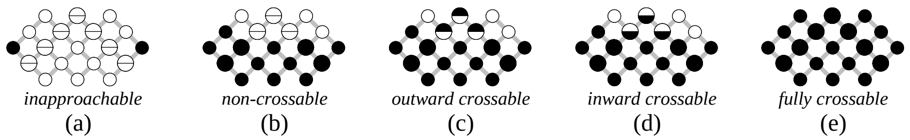

Fig. 12. Five types of regions' boundaries in terms of the movement patterns they accept.

7. Conclusion and Future Problems

This paper distinguished 26 topological DLine-region relations based on the 9^+-intersection. A conceptual neighborhood graph of these 26 relations took the shape of a V-shaped tube except one node. The 26 DLine-region relations qualitatively categorize the patterns of an agent's movement with respect to a region. It is a future question how to apply this model to the analysis of motional expressions in natural language (i.e., how people describes a movement), as well as the computer systems that communicate the information on spatial movement with human users, hopefully in a qualitative way.

In the current model, we can tell whether an agent crosses or touches the boundary, but cannot describe how many times the agent crosses or touches the boundary, or whether the agent crosses or touches the boundary instantly or stepwise. Also, we cannot describe, if the DLine and the region are disjoint, whether the agent goes left of, right of, toward, or against the region, even though people often emphasize such information when describing movement. It is, therefore, a future question to extend the current model in a meaningful way, incorporating other topological properties of DLine-region relations, such as the number and dimension (point or interval) of intersections, as well as non-topological properties such as distance and direction between the DLine and the region.

This paper did not discuss the composition of two DLine-region relations (Freksa 1992b; Egenhofer 1994). We can consider two types of compositions: the composition of two DLine-regions relations with a common DLine (i.e., all possible relations between two regions R_1 and R_2 when the relation between a DLine D and R_1 and the relation between D and R_2 are known) or that with a common region (i.e., all possible relations between two DLines D_1 and D_2 when the relation between D_1 and a region R and the relation between D_2 and R are known). The compositions of all pairs of 26 DLine-region relations yield two 26×26 composition tables, which will enrich the foundation of qualitative spatial reasoning.

The 9^+-intersection introduced in this paper provides a flexible and systematic framework for capturing topological relations between various spatial objects, including DLines, branching lines, regions with holes, and multi-component regions. The application of the 9^+-intersections for other spatial relations is highly potential for enriching the formal model of space configurations and the foundation of qualitative spatial reasoning.

Acknowledgments

This work was partially supported by the National Geospatial-Intelligence Agency in USA under grant number NMA201-01-1-2003 and NMA401-02-1-2009.

References

Alexandroff, P. (1961) *Elementary Concepts of Topology*. Dover, Mineola, NY.

Clementini, E. and Di Felice, P. (1998) Topological Invariants for Lines. *IEEE Transactions on Knowledge and Data Engineering*, **10**(1): 38-54.

Clementini, E., Di Felice, P., and van Oosterom, P. (1993) A Small Set of Formal Topological Relationships Suitable for End-User Interaction. in: Abel, D. and Ooi, B. C. (Eds.) *3rd International Symposium on Advances in Spatial Databases*, Singapore, Lecture Notes in Computer Science, 692, 277-295, Springer.

Egenhofer, M. (1989) A Formal Definition of Binary Topological Relationships. in: Litwin, W. and Schek, H.-J. (Eds.) *3rd International Conference on Foundations of Data Organization and Algorithms (FODO)*, Paris, France, Lecture Notes in Computer Science, 367, 457-472, Springer.

Egenhofer, M. (1994) Deriving the Composition of Binary Topological Relations. *Journal of Visual Languages and Computing*, **5**(2): 133-149.

Egenhofer, M. (2005) Spherical Topological Relations. *Journal on Data Semantics III*: 25-49.

Egenhofer, M. and Al-Taha, K. (1992) Reasoning About Gradual Changes of Topological Relationships. in: Frank, A., Campari, I., and Formentini, U. (Eds.) *Theories and methods of spatio-temporal reasoning in geographic space*, Pisa, Italy, Lecture Notes in Computer Science, 639, 196-219, Springer.

Egenhofer, M. and Franzosa, R. (1991) Point-Set Topological Spatial Relations. *International Journal of Geographical Information Systems*, **5**(2): 161-174.

Egenhofer, M. and Herring, J. (1991) Categorizing Binary Topological Relationships between Regions, Lines and Points in Geographic Databases. in: Egenhofer, M., Herring, J., Smith, T., and Park, K. (Eds.) *A Framework for the Definitions of Topological Relationships and*

an Algebraic Approach to Spatial Reasoning within This Framework, NCGIA Technical Reports 91-7. National Center for Geographic Information and Analysis, Santa Barbara, CA.
Egenhofer, M. and Mark, D. (1995a) Modeling Conceptual Neighborhoods of Topological Line-Region Relations. *International Journal of Geographical Information Systems*, **9**(5): 555-565.
Egenhofer, M. and Mark, D. (1995b) Naive Geography. in: Frank, A. and Kuhn, W. (Eds.) *COSIT '95*, Semmering, Austria, Lecture Notes in Computer Science, 988, 1-15, Springer.
Freksa, C. (1992a) Temporal Reasoning Based on Semi-Intervals. *Artificial Intelligence*, **54**: 199-227.
Freksa, C. (1992b) Using Orientation Information for Qualitative Spatial Reasoning. in: Frank, A., Campari, I., and Formentini, U. (Eds.) *The International Conference GIS - From Space to Territory: Theories and Methods of Spatio-Temporal Reasoning in Geographic Space*, New York, NY, Lecture Notes in Computer Science, 639, 162-178, Springer.
Hadzilacos, T. and Tryfona, N. (1992) Model for Expressing Topological Integrity Constraints in Geographic Databases. in: Frank, A., Campari, I., and Formentini, U. (Eds.) *The International Conference GIS—From Space to Territory: Theories and Methods of Spatio-Temporal Reasoning in Geographic Space*, New York, NY, Lecture Notes in Computer Science, 639, 252-268, Springer.
Hornsby, K., Egenhofer, M., and Hayes, P. (1999) Modeling Cyclic Change. in: Chen, P., Embley, D., Kouloumdjian, J., Liddle, S., and Roddick, J. (Eds.) *Advances in Conceptual Modeling*, Paris, France, Lecture Notes in Computer Science, 1227, 98-109, Springer.
Kurata, Y. and Egenhofer, M. (2006) The Head-Body-Tail Intersection for Spatial Relation between Directed Line Segments. in: *GIScience2006*, Münster, Germany, Lecture Notes in Computer Science, 4197, 269-286, Springer.
Kuratowski, K. (1930) Sur Le Probleme Des Courbes Gauches En Topologie. *Fundamenta Mathematicae*, **16**: 271-283.
Lynch, K. (1960) *The Image of the City*. MIT Press, Cambridge, MA.
Mark, D. and Egenhofer, M. (1994) Modeling Spatial Relations between Lines and Regions: Combining Formal Mathematical Models and Human Subjects Testing. *Cartography and Geographical Information Systems*, **21**(3): 195-212.
Moratz, R., Renz, J., and Wolter, D. (2000) Qualitative Spatial Reasoning About Line Segments. in: Horn, W. (Ed.) *14th European Conference on Artificial Intelligence*, Berlin, Germany, 234-238, IOS Press.
Papadias, D., Theodoridis, Y., Sellis, T., and Egenhofer, M. (1995) Topological Relations in the World of Minimum Bounding Rectangles: A Study with R-Trees. in: Carey, M. and Schneider, D. (Eds.), SIGMOD RECORD, 24(2), 92-103.
Schlieder, C. (1995) Reasoning About Ordering. in: Frank, A. and Kuhn, W. (Eds.) *COSIT '95*, Lecture Notes in Computer Science, 988, 341-349, Springer.
Schneider, M. and Behr, T. (2006) Topological Relationships between Complex Spatial Objects. *ACM Transactions on Database Systems*, **31**(1): 39-81.
Shariff, A., Egenhofer, M., and Mark, D. (1998) Natural-Language Spatial Relations between Linear and Areal Objects: The Topology and Metric of English-Language Terms. *International Journal of Geographical Information Science*, **12**(3): 215-246.
Talmy, L. (1996) Fictive Motion in Language and "Ception". in: Bloom, P., Peterson, M., Nadel, L., and Garrett, M. (Eds.) *Language and Space*. MIT Press, Cambridge, MA, 211-276.
Van de Weghe, N. and De Maeyer, P. (2005) Conceptual Neighbourhood Diagrams for Representing Moving Objects. in: *2nd International Workshop on Conceptual Modeling for Geographic Information Systems (CoMoGIS)*, Klagenfurt, Austria, Lecture Notes in Computer Science, 3770, 228-238, Springer.